Machine
GRAPHICS & VISION

International Journal

Application of Shape Analysis to the Assessment of Geometrical Properties of Grains in the Selected Species of Spring Cereals

Andrzej Borusiewicz [1], Paulina Drożyner [2]

[1] The Academy of Agrobusiness in Lomza, Department of Agronomy, Łomża, Poland,
andrzej.borusiewicz@wsa.edu.pl

[2] University of Warmia and Mazury in Olsztyn, Department of Foundations of Safety,
Olsztyn, Poland

Abstract. The competition in many branches of industry including agriculture has grown as a result of Polish access to the European Union. It resulted in the intense research development in order to intensify production processes and improve the quality of the final product. One of the methods which might be helpful in this process is the shape analysis. This method makes it possible to measure selected properties of materials in a very precise way. The paper presents the possibilities of computer analysis in the research of grain geometrical features of 128 species of cereals. The program ImageJ was used. It enabled us to define surface, perimeter, width, height and circular projection of every caryopsis. Shape analysis also helps to define basic values of the tested features of caryopsis species. Significant differences between the shape of tested cereals species were indicated. However, significant differences between varieties of the same species were not found. Barley grain had the largest average surface while rye grain had the smallest one. Winter barley grain had the largest perimeter and spring wheat had the smallest one. Oat was characterized by the longest average length while spring wheat had the smallest one. Winter barley had the largest grain width and rye had the smallest one. Spring wheat grain is the most circular while oat grain is the less circular one.

Taking into consideration the data mentioned above, one can use them in the production of equipment and machines used for seed planting, selection, segregation of cereal seeds both in agriculture as well as in agricultural and food processing industry.

Key words: caryopsis, spring cereals, grain, shape analysis, geometrical features.

1. Introduction and purpose of study

Cereals represents about 50% of world's crop production. What is more, they are the main ingredient of food due to high protein and carbohydrates content. They are also a valuable resource used in industry and for renewable energy ([18], p. 5-10). Due to large number of agricultural areas and moderate climate, Poland has a great potential in crop production, especially wheat production. It is willingly cultivated because its grain is rich in starches. Moreover, it contains the most protein and gluten in comparison with other crops [17].

After Polish access to the European Union the guarantee of specific crops parameters is an essential aspect in order to meet quality requirements concerning fresh and processed products and consequently consumer needs. The inspection of the processing and production and classification of a final product is necessary [11]. The access to the

European Union resulted in an increase in competition and demands for products with specific parameters. It forces manufacturers to obtain raw material of the most balanced technological parameters which guarantees efficient processing and obtaining the final product of the highest quality [3]. Thus, milling industry forces manufacturers to standardize raw material in terms of grain size as well as cereal growing of higher usability. Determination of optimal geometrical properties of grain cereals for processing makes it possible to search the relationships between grain size and its quality defining the features which influence the technological processes [6].

Geometrical features of the grain have a significant meaning during sorting, fragmentation and hulling of grain [2]. Caryopses can have different shape and a large variation of dimensions. Varieties of such features as size, shape, weight, moisture, colour and physical characteristics of grain occur between varieties even between one species. It is the result of biological differences, the place of maturation on a plant stem, cultivation techniques and soil and climate conditions [6]. Shape difference is a feature which is used in sorting and separation process. The shape of a single caryopsis has a relevant influence on total mixture of grain material, for example, it determines the angle of internal friction, the angle of dump response or decides about stress distribution in the mixture [8, 9]. This is the reason why the grain of standardized parameters have the highest technological value, and the most important feature is the even spread in length, width and thickness. Assessment of grain distribution having desirable features has the highest cognitive value and has a significant impact on cultivation [3].

The development of agriculture led to its intense automation. Processing and storage industry are the branches which dictate the requirements for engines, machines and equipment used for processing plant materials. Knowledge of physical features concerning processing of raw materials and their compounds which influence the interactions between the material and the technical system is necessary for proper machinery and equipment design. Such information is essential for high quality of a product and safe running of the processes [14].

Conventional and laboratory methods of plant materials assessment require much work and need expensive measuring equipment. This is the reason why modern measuring techniques which use image processing are becoming more and more popular in agri-food product quality testing [10, 5]. Nowadays computer vision techniques are used in many spheres of life, for example, in medicine and natural or engineering science. They are also used for supervising technological processes and assessment of object features. In agriculture they are used for inspection of the control in sorting and agricultural equipment and for the assessment of agricultural products quality. Identification of the features such as geometry, colours and surface structure with visual systems make it possible to detect the relationship between technological value of food materials and their external features. In the case of cereals the analysis concerns mainly the relationships between caryopsis dimensions, colour of seed cover, surface shape and gluten amount or

rheological features [7, 16]. The method of image analysis used in technology of grain
materials makes it possible to make a quantitative assessment of component distribu-
tion of grainy system mixture precisely. This method gives an opportunity to overcome
difficulties in assessment of grainy system mixing. A number of studies confirmed that
that mixed colours arrangement of components on the surface of mixer cross section
reflects empirical distributions of all the components of the whole volume which shows
the applicability of this method in assessment of grainy mixtures state [1, 12, 13].

2. Research methodology

The research was carried out in 2013. Geometrical features of 128 varieties of 5 crops
species were analysed. Cereal grains came from field experiments in COBORU (Experi-
mental Centre of Variety Assessment in Poland). The average level of farming technique,
basic mineral fertilization which take into account the type of soil, location and lodging
protection were used. In addition, two fungicide manipulations were used – in the phase
of full disseminating at the beginning of heading. The following varieties and species
were tested: 14 varieties of spring wheat, 31 varieties of winter wheat, 14 varieties of
rye, 6 varieties of spring rye, 25 varieties of winter rye, 9 varieties of oat, 19 varieties
of spring oat and 10 varieties of winter oat. All the tested varieties were listed in the
national register.

The features of 50 randomly selected caryopses of every variety were defined. The
computer program ImageJ [20] was used. Every sample of the variety were arranged in
10 rows: 10 pieces which are reversed with furrow to scanner screen. The seeds were
put on a white background. They had the same dimension for every test. Having taken
a picture, they were analysed with a computer program consisting of determination of
such geometrical parameters as surface, perimeter, length, width and circularity of every
caryopsis. The obtained data were analysed using statistical methods. Statistical mea-
sures such as average, minimum, maximum, standard deviation, coefficient of variation,
correlation and regression were calculated. The obtained results of grain were compared
with their yielding in order to choose the most favourable variety.

3. Results and discussion

Winter Barley
The variety Nickela had the largest surface of grain among tested varieties of winter
barely while the variety Skarpia had the smallest one (Tab. 1). It must be said that the
caryopses of tested varieties demonstrated quite aligned parameters of tested geometrical
features. However, essential differences in distribution of tested features have not been
found. The variety Holmes had the highest average grain yield 77.5 dt/ha. The variety
Nickela had the largest average level of 60 dt/ha while the variety Skarpia with the

smallest caryopsis had 55 dt/ha. The variety Fridericus 49.9 dt/ha had the smallest yield.

Spring Barley

Among the tested varieties of spring barley no essential differences were found (Tab. 2). The variety Gawrosz had the smallest caryopsis among tested varieties while the variety Despina had the most aligned one with regard to the tested geometrical features. During a field experiment the variety Ella 64.8 dt/ha demonstrated the highest average yield while the variety KWS Orphelia had the lowest one 51 dt/ha. The variety Despina achieved yield of 59.2 dt/ha and the variety Gawrosz 52.7 dt/ha.

Oat

As for the tested varieties of oat, the variety Bingo had the largest surface of grain while the variety Nogus had the smallest one (Tab. 3). At the same time the variety Nogus had the most circular grain among all the tested varieties of oat. During a field experiment the variety Bingo had the highest grain yield 57.4 dt/ha and the varieties Siwek (44.6 dt/ha) and Nagus 44.5 dt/ha had the lowest ones.

Spring wheat

Among the tested varieties of spring wheat the largest area of grain surface Parabola variety had the largest surface and Trappe had the smallest one (Tab. 4). During a field experiment the Tybalt variety 75 dt/ha had the largest average yield growth whereas the variety Ostka Smolic 58.4 dt/ha had the smallest one. The varieties of Parabola and Trappe achieved yield at the similar level 66.4 dt/ha and 67 dt/ha.

Tab. 1. Average values of geometrical features concerning winter barley varieties with grain yield.

	Surface [cm²]	Perimeter [cm]	Length [cm]	Width [cm]	Circularity	Grain yield dt/ha
Antonella	0.1145	1.5545	0.6453	0.2491	0.6009	58.4
Holmes	0.1242	1.6484	0.6767	0.2653	0.5835	77.5
Nickela	0.1353	1.5934	0.639	0.2923	0.673	60
Skarpia	0.1037	1.4285	0.5857	0.239	0.6408	55
Karakan	0.1196	1.6441	0.6977	0.2414	0.562	37.4
KWS Meridian	0.1103	1.5558	0.6504	0.2395	0.5807	65
Souleyka	0.1192	1.5785	0.65	0.2561	0.613	65.6
Titus	0.1109	1.5553	0.6548	0.2356	0.5806	65.5
Henriete	0.1148	1.5202	0.6289	0.2487	0.6258	51.1
Fridericus	0.118	1.5597	0.6438	0.2551	0.6148	49.9

Tab. 2. Geometrical values of winter barley caryopsis.

	Surface [cm²]	Perimeter [cm]	Length [cm]	Width [cm]	Circularity	Grain yield dt/ha
Natasia	0.1037	1.4285	0.5857	0.239	0.6408	52.7
Despina	0.1081	1.4099	0.5669	0.26	0.685	59.2
Gawrosz	0.09	1.2618	0.5066	0.2355	0.7125	52.7
Skald	0.1056	1.3778	0.55	0.2561	0.6992	60
Gooluck	0.1041	1.3651	0.5445	0.2558	0.7012	60
Mercada	0.1079	1.4048	0.5623	0.2562	0.6874	52
KWS Atrika	0.107	1.3871	0.5538	0.2576	0.6995	53.8
Iron	0.0992	1.3474	0.5419	0.2481	0.6867	51.9
KWS Aliciana	0.1018	1.3602	0.5437	0.2532	0.6933	54.6
Ella	0.1035	1.37	0.5484	0.2574	0.6926	64.8
Basic	0.1033	1.3696	0.5494	0.254	0.6937	53.1
Fariba	0.0964	1.3332	0.5385	0.2443	0.6822	52.4
KWS Orphelia	0.0936	1.2747	0.5038	0.2493	0.7239	51
Suweren	0.1034	1.3936	0.5654	0.2483	0.6712	58.9
Raskud	0.1009	1.3537	0.5438	0.2507	0.6932	60.6
Soldo	0.0981	1.3493	0.546	0.2438	0.6771	59.1
Conchita	0.1068	1.4072	0.5658	0.258	0.681	57.2
Skald	0.1016	1.3623	0.5457	0.2526	0.6884	60
Kucyk	0.0996	1.3203	0.5221	0.2552	0.7179	65.5

Tab. 3. Average individual features of oat varieties grain.

	Surface [cm²]	Perimeter [cm]	Length [cm]	Width [cm]	Circularity	Grain yield dt/ha
Gniady	0.1114	1.516	0.6367	0.2276	0.6055	55.6
Haker	0.1133	1.6367	0.709	0.2076	0.5298	54.8
Zuch	0.1176	1.734	0.76	0.2068	0.4912	45.1
Siwek	0.0835	1.3487	0.5681	0.1979	0.5893	44.6
Nogus	0.067	1.1426	0.4694	0.1809	0.6457	44.5
Krezus	0.1161	1.6097	0.689	0.2252	0.5646	53
Arden	0.1201	1.6937	0.7343	0.2182	0.5283	55.8
Maczo	0.0868	1.363	0.5729	0.1964	0.5914	46.1
Bingo	0.1218	1.7336	0.7489	0.2293	0.5083	57.4

Tab. 4. The average values of geometrical parameters of spring wheat.

	Surface [cm^2]	Perimeter [cm]	Length [cm]	Width [cm]	Circularity	Grain yield dt/ha
Kandela	0.0775	1.0845	0.3962	0.243	0.826	67.4
Radocha	0.0855	1.1351	0.41	0.2544	0.8314	72.9
Hewilla	0.0761	1.0678	0.3871	0.2423	0.8363	65
Izera	0.0812	1.1149	0.4103	0.2473	0.8195	72.5
Tybalt	0.0846	1.139	0.4211	0.2506	0.8167	75
KWS Torridon	0.0757	1.0697	0.3907	0.2398	0.8296	65.2
Monsun	0.0812	1.1149	0.4103	0.2473	0.8195	64.7
Trappe	0.0657	0.9946	0.3635	0.2249	0.8316	66.4
Łagwa	0.078	1.0768	0.3866	0.2472	0.8437	70.5
Parabola	0.095	1.2101	0.4445	0.263	0.8147	67
Arabeska	0.0742	1.0436	0.3681	0.2481	0.8533	68
Katoda	0.0735	1.0509	0.3772	0.2399	0.8347	63.6
Ostka Smolnic	0.075	1.0734	0.3947	0.2347	0.8165	58.4
SMH 87	0.0856	1.2236	0.4672	0.2258	0.727	68.3

Winter wheat

Among the tested varieties of winter wheat the Komnata variety had the largest area of surface and perimeter of grains while the Garantus variety had the smallest one (Tab. 5). The variety of Garantus has the best circularity of grains. The Jantarka variety had the most similar values of measured geometrical features of grains. During a field experiment the Fidelius variety 88.7 dt/ha had the largest average yield growth whereas Komnata had the smallest one, the hard wheat variety, 48.1 dt/ha and the Belenus variety 58.4 dt/ha. The Garantus variety achieved yield at the level of 75.1 dt/ha and the Jantarka variety 72.5 dt/ha.

Spring triticale

Among the tested varieties of spring triticale the largest area of surface was found in the varieties of Milkaro and Anrus, the smallest one – in the Bojko variety (Tab. 6). The grain of the Andrus variety had the largest perimeter while the Bojko variety was characterized by the smallest grain circularity. Milkaro is a spring triticale variety which emphasizes the most general features of the appropriate grain image. In the experimental field the highest yield was obtained by the varieties of Andrus 58 dt/ha and Nagano 57.7 dt/ha, whereas the lowest yield was obtained by the Milkaro variety 52.5 dt/ha.

Tab. 5. The average values of geometrical parameters of winter wheat.

	Surface [cm²]	Perimeter [cm]	Length [cm]	Width [cm]	Circularity	Grain yield dt/ha
Kranich	0.0727	1.0528	0.3856	0.2349	0.822	75
Fidelius	0.0807	1.1019	0.4024	0.2488	0.8329	88.7
Skagen	0.0782	1.082	0.3916	0.2437	0.8373	69.8
Mulan	0.0777	1.0829	0.397	0.2417	0.8313	72.6
Figura	0.0755	1.069	0.3916	0.2401	0.8296	70.9
Torrild	0.0773	1.0745	0.3873	0.2444	0.8391	73.4
Kohelia	0.0858	1.1432	0.4229	0.2502	0.8225	75.8
Markiza	0.076	1.0728	0.3958	0.236	0.8265	72.7
Natula	0.0797	1.0963	0.403	0.245	0.8318	71.9
Meteor	0.076	1.066	0.3827	0.245	0.8381	65.1
Sailor	0.0766	1.0642	0.3824	0.2464	0.8488	73.3
Bockris	0.0789	1.0872	0.3973	0.2451	0.8364	71.5
Linus	0.0834	1.123	0.4104	0.2494	0.8291	75.1
Elipsa	0.0791	1.0912	0.3941	0.2459	0.8329	78.1
Komnata	0.1021	1.3152	0.5122	0.2464	0.7414	48.1
Satyna	0.0759	1.0845	0.4062	0.2305	0.8092	66.8
Forkida	0.0817	1.1084	0.4011	0.2516	0.8337	75
KWS Ozon	0.078	1.0858	0.3963	0.2414	0.8288	75.3
Garantus	0.0667	0.9887	0.3489	0.2359	0.8563	75.1
Bogatka	0.0839	1.1261	0.4108	0.2551	0.8306	75.8
Bystra	0.079	1.0868	0.3905	0.2478	0.8399	70.9
Jantarka	0.0917	1.1773	0.4304	0.2629	0.8303	72.5
Bamberka	0.0881	1.1416	0.4078	0.2643	0.848	59.7
Ostroga	0.0917	1.1703	0.4187	0.2681	0.84	66
Meister	0.0906	1.1756	0.4335	0.2553	0.8212	67
Oxal	0.0854	1.1339	0.4129	0.2539	0.8317	70.2
Smaragd	0.0811	1.095	0.3898	0.2535	0.8472	76.1
KWS Dacanto	0.0853	1.1316	0.4089	0.2543	0.8352	76.8
Arkadia	0.0849	1.137	0.4189	0.2496	0.8231	73.7
Muszelka	0.0844	1.1238	0.409	0.2522	0.8374	67
Belenus	0.0694	1.0264	0.3743	0.2299	0.8244	58.4

Tab. 6. The average values of geometrical parameters of some varieties of spring triticale grains.

	Surface [cm²]	Perimeter [cm]	Length [cm]	Width [cm]	Circularity	Grain yield dt/ha
Nagano	0.0875	1.2059	0.4666	0.2372	0.7529	57.7
Andrus	0.0994	1.3414	0.5368	0.2369	0.6925	58
Mieszko	0.0869	1.2303	0.485	0.2279	0.7189	53.8
Milkaro	0.0999	1.3159	0.518	0.2448	0.7227	52.5
Milewo	0.0938	1.2872	0.5131	0.2314	0.709	53.4
Dublet	0.0909	1.2354	0.4834	0.2364	0.7463	55.4

Winter triticale

Among the tested winter triticale varieties the largest area of grain surface was found in the Algoso and Borowik varieties, the smallest one – in the Bereniko variety. Furthermore, the varieties of Algoso and Borowik had the largest grain perimeter. The largest average grain yield was registered for the KWS Trisol 86.7 dt/ha, the Pigmej short–stem variety, 83.5 dt/ha and the Agostino short-stem variety, 82 dt/ha. The lowest yield was obtained by the Pizarro variety, on the average by 63.4 dt/ha and the Leontino variety, 61.5 dt/ha.

Rye

Among the tested rye varieties the varieties of Armand and Brasetto had the largest area of grain surface, while the smallest one – the Domir variety (Tab. 7). The varieties of Armand and Brasetto had the largest grain perimeter. The length of examined grains as well as their width show a little difference between them. In the experimental field the largest average yield characterised the hybrid varieties: Brasetto 78.3 dt/ha, Visello 72.9 dt/ha and Gonello 72.6 dt/ha, whereas the smallest one – the Bosmo variety 54.6 dt/ha and the Herakles variety 54.8 dt/ha. The Armand variety achieved yield at the level of 60.7 dt/ha and the Domir variety 60.2 dt/ha.

The development of digital techniques extends the abilities to process the picture. Using fast processes makes it possible to carry out multilateral activities in order to interpret and make the most of the acquired picture [8]. The computer analysis allows us to bring the numerical information to the light in a very efficient and precise way, which gives the fast, repetitive and objective assessment of the grain quality. It is becoming more and more common in the plant production as claimed by Guzek in [19]. Diversity of geometrical features: area of surface, perimeter, width, length and circularity describing the shape of grains, makes it possible to use computer image analysis techniques to identify the cereal grains, as claimed by Zapotoczny in [16]. The role of digital image analysis in the grain materials technology is very significant. The colour characteristics

Tab. 7. The average values of geometrical parameters of some varieties of winter triticale grains.

	Surface [cm^2]	Perimeter [cm]	Length [cm]	Width [cm]	Circularity	Grain yield dt/ha
Borwo	0.0852	1.1699	0.449	0.2397	0.7798	79.5
Gniewko	0.0853	1.1779	0.4559	0.2379	0.7707	74.2
Tulus	0.0961	1.303	0.5218	0.2384	0.7103	76.8
Algoso	0.1077	1.3493	0.532	0.2551	0.7416	76.7
Pizarro	0.1019	1.3088	0.5144	0.2527	0.7461	63.4
Mikado	0.0898	1.2429	0.494	0.2316	0.7283	73.7
Borowik	0.1076	1.3671	0.5407	0.2503	0.7218	79.4
Moderato	0.0788	1.1386	0.441	0.227	0.7628	69.9
Sorento	0.0909	1.2787	0.5133	0.2257	0.697	76.6
Elpaso	0.0773	1.1482	0.4521	0.2211	0.7352	81.4
Leontino	0.0855	1.1865	0.4612	0.2348	0.7598	61.5
Pawo	0.0861	1.1944	0.4673	0.2389	0.7582	71.2
Fredro	0.079	1.1413	0.4428	0.2273	0.7612	72.9
Cerber	0.093	1.2724	0.5039	0.2404	0.721	77.6
Maestozo	0.0905	1.263	0.5071	0.2262	0.7119	70.4
Bereniko	0.0765	1.0969	0.4161	0.2307	0.7976	68.8
Baltiko	0.0886	1.233	0.4892	0.2303	0.7316	75.4
Atletico	0.094	1.249	0.4911	0.2408	0.7554	75.7
Grenado	0.089	1.2245	0.485	0.239	0.7449	81.1
Alekto	0.0877	1.197	0.4645	0.2389	0.7678	68.3
Cyrkon	0.0962	1.2983	0.5152	0.2419	0.7161	75.4
Agostino	0.0901	1.2243	0.4804	0.2393	0.7543	82
Witon	0.0784	1.1357	0.441	0.2288	0.7618	76.7
Pigmej	0.0847	1.1988	0.4731	0.2265	0.7374	83.5
KWS Trisol	0.1004	1.3123	0.5191	0.2516	0.7308	86.7

Tab. 8. The average values of geometrical parameters of rye grains.

	Surface [cm^2]	Perimeter [cm]	Length [cm]	Width [cm]	Circularity	Grain yield dt/ha
Brasetto	0.0733	1.1508	0.4635	0.2015	0.6938	78.3
Armand	0.0748	1.1606	0.4604	0.2091	0.6968	60.7
Dańk. Diament	0.0687	1.0854	0.428	0.2027	0.7311	62.7
SU Skaltio	0.0686	1.1146	0.4498	0.1909	0.6944	67.7
Dańk. Amber	0.0687	1.1091	0.4466	0.1956	0.7017	58.8
Visello	0.0707	1.1267	0.4551	0.1993	0.6977	72.9
Palazzo	0.067	1.0938	0.4368	0.1962	0.7027	64.4
SU Drive	0.067	1.0938	0.4368	0.1962	0.7027	66.2
Bosmo	0.0697	1.1229	0.4537	0.1943	0.694	54.6
Stanko	0.0673	1.0955	0.4403	0.1948	0.7037	67.2
Domir	0.0659	1.0757	0.4237	0.2038	0.7149	60.2
Minello	0.0667	1.0917	0.4411	0.1923	0.7025	68.9
Horyzo	0.0707	1.1217	0.4507	0.1964	0.7046	65.2
Gonello	0.0707	1.1382	0.4642	0.1915	0.6837	72.6

Tab. 9. The finished average results of the geometrical crop species.

	Surface [cm^2]	Perimeter [cm]	Length [cm]	Width [cm]	Circularity
Winter triticale	0.0896	1.2285	0.4829	0.2366	0.7441
Spring triticale	0.0916	1.2675	0.502	0.2315	0.7144
Rye	0.0693	1.1156	0.4479	0.1977	0.6994
Spring wheat	0.0776	1.0876	0.3971	0.2417	0.8236
Winter wheat	0.0812	1.1069	0.4037	0.2474	0.8302
Oats	0.1042	1.5309	0.6542	0.21	0.5616
Winter barley	0.1171	1.5638	0.6472	0.2522	0.6075
Spring barley	0.1011	1.3555	0.5432	0.2509	0.6925

of homogeneous grain system was found to be a great way to estimate the quantity of decay of mixed components. The above described method solves the problem of rating the mixing of grain systems [15]. The knowledge about the physical features of cereal products allows to assess their technological quality for consumption or feeding. Besides, the seed dimensions and shape refer to the endosperm or other parts of the grain (e.g. covering), and make it possible to describe the milling value of seeds. A system based on the digital image analysis can fulfill a function of estimating the quality of seeds in the storage, for the business trading and in the material preparing processes for milling. The scheme of geometrical features can help to build the basis of models, describing the agricultural properties of examined varieties.

4. Conclusions

- Using the digital shape analysis made it possible to obtain the accurate survey of examined geometrical values: area of surface, perimeter, length, width and circularity of grains.

- The crop with the largest area of grain surface and perimeter is winter barley. Not only for this reason it takes the first place, but it also has the widest seeds among the rest of crops. The longest grains are found in oats – 0,6542 cm. The best grain circularity is found in winter triticale – 0,8302 cm. The smallest values of the grain perimeter – 1,0876 cm, and the grain width – 0,3971 cm are found in spring wheat. It is the same with the grain heights of that crop – 1977 cm. Oats have very weak grain circularity – 0,5616 cm, mainly due to the typical kind of surface.

- It is observed that there is a relationship between the received data from the shape analysis of grains and the grain yield of crops.

- The computer image analysis makes it possible to determine the parameters of agricultural equipment and machines with great precision: seed drills, combines, crushers for feed stuff production and mills of the 21st century.

References

2000

[1] Matuszek J., Plinta D.: System komputerowego wspomagania projektowania procesów wytwarzania "SYSKLASS". Politechnika Łódzka, Filia w Bielsku-Białej.

2003

[2] Dziki D., Laskowski J.: Wpływ cech geometrycznych ziarna pszenicy na właściwości mechaniczne i podatność na rozdrabnianie. Acta Agrophysica 2(4):735-742.

[3] Geodecki M., Grundas S.: Charakterystyka cech geometrycznych pojedynczych ziarniaków pszenicy ozimej i jarej. Acta Agrophysica 2(3):531-538.

[4] Puczel. B.(red.), Gazda W.: Wyniki Porejestrowych doświadczeń odmianowych i rolniczych zbóż, grochu siewnego, kukurydzy, ziemniaków. COBORU, SDOO w Krzyżewie. Porejestrowe Doświadczalnictwo Odmianowe i Rolnicze.

[5] Tukiendorf, M. Characteristics of mixing granular materials achieved by using methods of variance analysis and geostatistical functions. Electronic Journal of Polish Agricultural Universities, 6(1).

2005

[6] Hebda T., Micek P.: Zależności pomiędzy właściwościami geometrycznymi ziarna zbóż. Inżynieria Rolnicza 6:233-240.

[7] Zapotoczny P.: Wpływ rozdzielczości i kompresji obrazu na błąd pomiaru geometrii oraz barwy ziarniaków zbóż. Inżynieria Rolnicza 8:417.

2006

[8] Frączek J., Wróbel M.: Metodyczne aspekty oceny kształtu nasion. Inżynieria Rolnicza 12(87):155-163.

[9] Frączek J., Slipek Z.: Modele roślinne struktur ziarnistych. Inżynieria Rolnicza 12(87):145-154.

2007

[10] Matuszek D., Tukiendorf M.: Komputerowa analiza obrazu w ocenie mieszania niejednorodnych układów ziarnistych (system funnel-flow). Inżynieria Rolnicza, 2(90):183-188.

[11] Tukiendorf M., Rut J., Szwedziak K.: Disintegration of storing the temperature of a grain of wheat in the time. Inżynieria Rolnicza, 9(97):247-252

2008

[12] Mleczko J.: Komputerowe wspomagania planowania przebiegu procesów produkcyjnych. Wydawnictwo Fundacji Centrum Nowych Technologii, Bielsko-Biała.

[13] Mleczko J.: Komputerowo wspomagane zarządzanie wytwarzaniem. Wydawnictwo Fundacji Centrum Nowych Technologii, Bielsko-Biała.

2009

[14] Frączek J., Wróbel M.: Zastosowanie grafiki komputerowej w rekonstrukcji 3D nasion. Inżynieria Rolnicza 6(115):87-94.

[15] Rut J., Szwedziak K.: Komputerowa analiza obrazu w ocenie mieszania jednorodnej mieszaniny ziarnistej. Inżynieria Rolnicza 9:207-208.

[16] Zapotoczny P.: Dyskryminacja odmian pszenicy na podstawie cech geometrycznych. Inżynieria Rolnicza 5:319-327.

2010

[17] Ginter A., Szarek S.: Sytuacja dochodowa producentów zbóż na przykładzie uprawy pszenicy. Journal of Agribusiness and Rural Development, 4(18):29-39.

2011

[18] Arseniuk E., Oleksiak T.: Dlaczego zboża. Poradnik dla producentów. Agro Serwis. Wydanie V.

[19] Guzek D., Wierzbicka A., Głąbska D.: Potencjał oraz zastosowanie komputerowej analizy i przetwarzania obrazu w przemyśle rolno-spożywczym. Inżynieria Rolnicza, 4:67-71.

2012

[20] Ferreira T., Rasband W.: ImageJ user guide. Available online form `imagej.nih.gov/ij/`→`docs`. Accessed 2012.12.10.

Hough Transform for Lines
with Slope Defined by a Pair of Co-primes

Leszek J Chmielewski, Arkadiusz Orłowski

Faculty of Applied Informatics and Mathematics (WZIM)
Warsaw University of Life Sciences (SGGW)
Nowoursynowska 159, 02-775 Warsaw, Poland
{leszek_chmielewski,arkadiusz_orlowski}@sggw.pl
http://www.wzim.sggw.pl

Abstract. Data structure and Hough-type algorithm suitable for finding the lines having the slope exactly specified by the ratio of small co-prime numbers is proposed. It is suitable for analysing images like the Ulam square in which the points representing prime numbers form such structures as contiguous lines and other regular sequences of points. This analysis is different from that in the case of images in which the real-world objects are represented approximately. Until now in the Ulam square the horizontal and vertical sequences, and those inclined by 45 deg were typically analysed. With the proposed method the sequences having slopes represented by such tangents like 1/3, 2/3, 3/4 etc. can be looked for.

Key words: Hough transform, slope, co-prime, coprime, prime, Ulam, square, spiral.

1. Introduction

The Hough transform has its long history coming back to the first conference paper of P.V.C. Hough [1] and his frequently cited patent [2]. Since the paper by Duda and Hart [4] recapitulated the concept of the Hough transform, it gained large interest and was further developed by numerous authors, as described in the review paper [6]. After the next review [7] was published, a long break in publishing the state-of-the-art reviews in this domain seemed to appear, excluding some internal reports like for example [11].

The problem of our interest is the case of exact digital lines like those present in the Ulam spiral [3]. The central part of the Ulam spiral embedded in the Ulam square is shown in Fig. 1. The points in the square have coordinates (p, q) having the origin in the starting number 1 of the spiral. the image of an $U \times U = 51 \times 51$ square with the embedded Ulam spiral containing $P = 378$ primes, where the largest one is 2593, is shown in Fig. 2. In this picture some sequences of pixels which form lines can be seen, for example, the lines marked green and red. Please note that these are not the digital representation of continuous lines, but rather the regular sequences of pixels in which the increments of the two coordinates are co-primes. The term *line* will be considered here as equivalent to such type of a *sequence*. The meaning of the lines visible in the Ulam spiral were widely discussed (see for example [8], with the references to more literature).
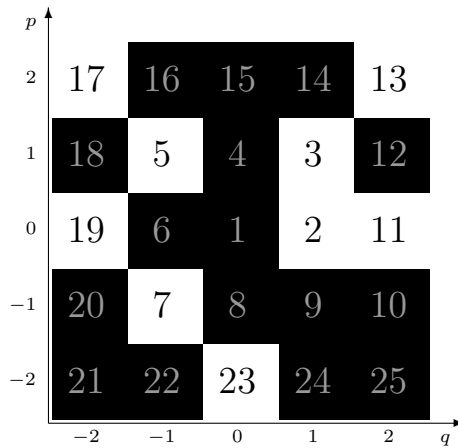
Fig. 1. The central part of the Ulam spiral for dimensions 5×5. Here, (p, q) represent coordinates in the square. Primes: black on white background, other numbers: grey on black.
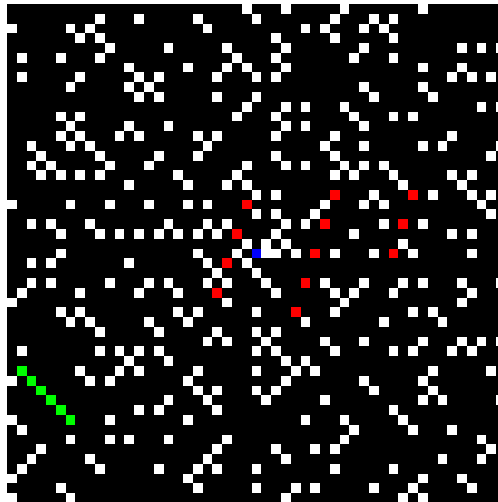

Fig. 2. Ulam spiral restricted to 51×51 pixels. Blue pixel corresponds to the spiral origin corresponding to number 1. White, red and green pixels are primes. Green pixels correspond to a line segment which form a line with slope $(\Delta p, \Delta q) = (1, -1)$ and red ones to three line segments inclined by $(3, 1)$, of different lengths.
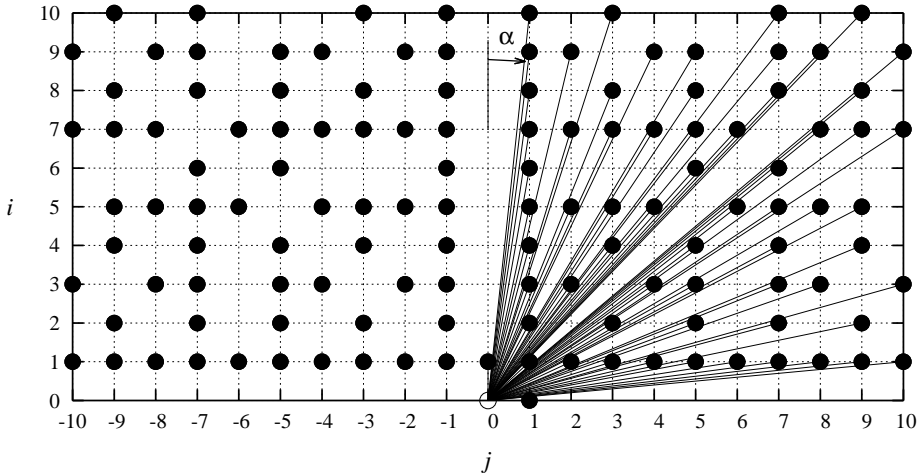
Fig. 3. Directional vectors represented with table of directions D_{ij} containing increments $(\Delta p, \Delta q) = (i, j)$. Each vector has the initial point at the empty circle $(0, 0)$ and the terminal point in one of the black circles (i, j), $\neg(i = 0 \wedge j = 0)$. α is the angle between the line segment and the vertical axis.

However, here we shall not consider this meaning. Rather, we shall concentrate solely on the data structure and organisation of the Hough-type algorithm which supports the detection of such lines, or sequences.

In the case considered the directions are restricted to those accurately represented by ratios of co-prime numbers. In the literature a data structure loosely related to such a case has been proposed by Wallace [5]. As described in [6], the line was parameterized by its two intersections with the perimeter of the image, and it was claimed that all the lines which can be drawn in the image can be represented in this way. This interesting idea is not adequate for our case, so a different structure will be proposed.

2. Structure of the accumulator

2.1. Representation of direction

The direction will be represented directly with two numbers which represent the increments of the coordinates between the subsequent points of the sequence, like for example those shown in Fig. 2 with red pixels, having the slope represented by $(\Delta p, \Delta q) = (3, 1)$. In Fig. 3 the direction table D_{ij} indexed by (i, j) which represent increments $(\Delta p, \Delta q)$ of coordinates p, q from Fig. 1. Only such pairs for which i, j are co-primes represent

different slopes; other pairs are redundant. Each index belongs to the set $[-N, N] \cap \mathcal{C}$ and here it was assumed that $N = 10$. For the sake of equivocality $i \geq 0$.

It is evident that only a small number of angles can be represented. The relation of the coordinates in the direction table and the angles α formed by the directional vector and the vertical axis can be seen in Fig. 3.

2.2. Representation of offset

The offset of horizontal lines is represented by the intercept with the vertical axis p, that of other lines by the intercept with the horizontal axis q. For a given slope, the intercepts for different lines can differ only by a unit, so they can be easily represented by an integer index k. The choice of such an index is secondary. For example, it can be the smallest nonnegative index q of the point belonging to the line, or the intercept with the axis q rounded down.

2.3. Representation of a line and the accumulated value

A line in the square is represented by a triple of indexes (i, j, k). As shown in Fig. 4, from the array of directions only the co-prime pairs (i, j) have the data accumulated, so only for them the data along the axis k should be assigned. The set of data accumulated along k can be organized as a table or a list of elements. The table is more convenient when the number of data to be accumulated can be estimated before the calculations. Otherwise, the list is recommended, but it consumes more memory due to the need of storing the pointers. In our case, the number of data is equal to the number of different values of index k which can be easily determined from the dimensions of the Ulam square.

The last element to be determined is what data are accumulated. In the case of our concern, the points in the Ulam square corresponding to primes are considered, and the natural choice of the Hough transform type is the two-point transform, because the elemental subset (cf. [9, 10]), that is the set of points for which the line slope and the intercept can be determined, is a pair of points. Therefore, pairs of points are accumulated in the elements of the tables indexed by k. For the sake of further analysis, the pairs themselves should be stored also, which makes it necessary for each accumulator element to contain a list of such pairs. The memory requirements for the analysis are large, as it is usually the case for Hough transform. Pairs (i, j) belong to a small set with cardinality $|\{(i, j)\}| \ll N^2$ which can be considered constant. Therefore, the accumulator can be considered as three-dimensional.
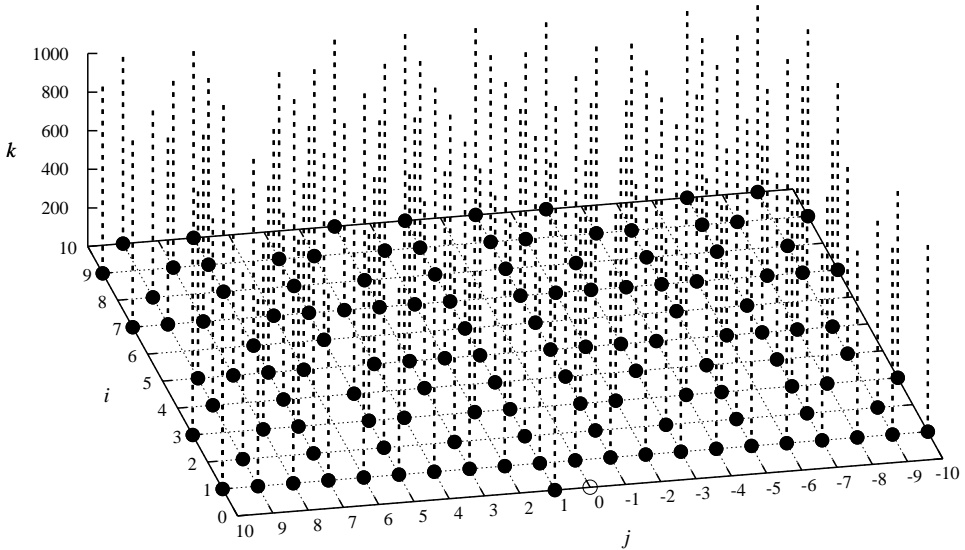
Fig. 4. Directions (i, j) together with offset index k represented in the accumulator. Along the coordinate k the accumulator can be organized as a table or as a list.

3. Accumulation and analysis of results

The data points in the Ulam square are the prime numbers which form the Ulam spiral. As it has already been mentioned, the voting subset of the set of prime points is a pair of such points. At least two strategies of forming such pairs are possible.

The local strategy is that due to the limit on directions determined by the size of the direction array D specified by N, for each prime point, its neighbours in the square at Manhattan distance up to N should be checked for the existence of a second prime point. Due to symmetry in the pair, only a half (roughly) of this neighbourhood should be checked, for example, if the square is analysed from left to right and from top to bottom, then the second points in the same verse to the right of the first point, and all those under the first point. The number of these points is proportional to N^2, so the number of pars is proportional to PN^2. In this way, if the sequence or line containing prime points which are mutually farther from each other than N can not be detected. Consequently, the prime points which are isolated on a line in the sense of this distance are never accumulated. The complexity of the accumulation algorithm is $O(PN^2)$.

The global strategy is, for each point in the sequence of the Ulam spiral, being the first point of the voting subset, to consider each other point located further in the Ulam spiral. For this, it is necessary to have the spiral stored as an ordered set of prime points,

each with its index, prime value and coordinates (p, q). Then, the number of voting pairs is $P(P - 1)/2$ and the complexity of the accumulation algorithm is $O(P^2)$. The lines, or sequences of prime points at arbitrary mutual distance inside the Ulam square, but with slopes limited to those represented by D, can be detected in this way.

After the accumulation, each accumulator element (i, j, k) contains a set of pairs of prime points which all belong to a line inclined by (i, j) and with offset determined by k. The pairs can be easily transformed into the ordered set of prime points, each with its index, prime value and coordinates (p, q). The number of prime points and the number of pairs for the current line is stored. Both in the case of the global and local strategy of accumulation, the continuity condition of the subsequent points in the ordered set of points can be tested to find the contiguous subsets of points in the lines, or the subset forming the other conditions of choice.

4. Example of results for a test case: square 5×5

To make it possible to understand the results shown further, let us consider a simple example for which the results can be explicitly presented in detail. To this end let us consider a small Ulam square 5×5, shown in Fig. 1. It seems to be the smallest square in which the results are not too trivial to exemplify the action of the algorithm. A file with results for this spiral is shown in detail in the listing in Fig. 5. The results shown in this listing can be visually presented in the graphs shown in Fig. 6. Some of the known features of the Ulam spiral can be seen even in such a small square. For example, at the directions $\alpha = -45°, 0°, 45°, 90°$ the numbers of lines, primes on these lines and primes per line are nearly always larger than those for the other angles.

5. Conclusion and future prospects

The data structure and the algorithm based on the Hough transform principle suitable for finding the lines, or the sequences of points, having the slope specified exactly by the ratio of co-prime numbers, was proposed. This data structure and algorithm make it possible to analyse the images like the Ulam square, in which the points which represent prime numbers form such structures as contiguous lines and other regular sequences of points. Such sequences should be analysed in the exact way. The exactness of this analysis makes it different from that for images in which the real-world objects are represented in an approximate way.

Until now the sequences with slope described $(0, 1)$ or $(1, 1)$ in the Ulam square were investigated. With the proposed method, more complex sequences like those described with slopes $(1, 3), (2, 3), (3, 4)$ etc. can be looked for. Configurations of points other than continuous point sequences can be studied.

```
# Unsorted lines through 5*5 spiral square
# 25 numbers, among them 9 primes
5  25  9

# list of all 25 numbers; among them the 9 primes have at least one nonzero coordinate
 1[0,0] 2[0,1] 3[1,1] 4[0,0] 5[1,-1] 6[0,0] 7[-1,-1] 8[0,0] 9[0,0] 10[0,0] 11[0,2] 12[0,0] 13[2,2]
 14[0,0] 15[0,0] 16[0,0] 17[2,-2] 18[0,0] 19[0,-2] 20[0,0] 21[0,0] 22[0,0] 23[-2,0] 24[0,0] 25[0,0]

#(<direction>) <number of its lines> <number of its prime points>:
#  <number of primes in a line>: <list of primes in a line>
(  0,1  )              3              7:
    2: 17 13
    2: 3 5
    3: 11 19 2
(  1,-3 )              2              4:
    2: 3 17
    2: 11 5
(  1,-2 )              2              4:
    2: 11 17
    2: 2 5
(  1,-1 )              3              7:
    2: 3 11
    2: 5 17
    3: 7 19 23
(  1,0  )              4              8:
    2: 11 13
    2: 2 3
    2: 5 7
    2: 17 19
(  1,1  )              3              7:
    2: 11 23
    3: 7 3 13
    2: 19 5
(  1,2  )              2              4:
    2: 2 7
    2: 13 19
(  1,3  )              3              6:
    2: 11 7
    2: 3 19
    2: 13 5
(  2,-3 )              1              2:
    2: 17 2
(  2,-1 )              1              2:
    2: 23 17
(  2,1  )              1              3:
    3: 23 2 13
(  3,-1 )              2              4:
    2: 5 23
    2: 17 7
(  3,1  )              1              2:
    2: 23 3

# Found 28 lines.
# Maximum number of primes 3 found in line at direction (0,1) through prime 2[0,1].
# Maximum number of primes 8 found at direction (1,0).
```
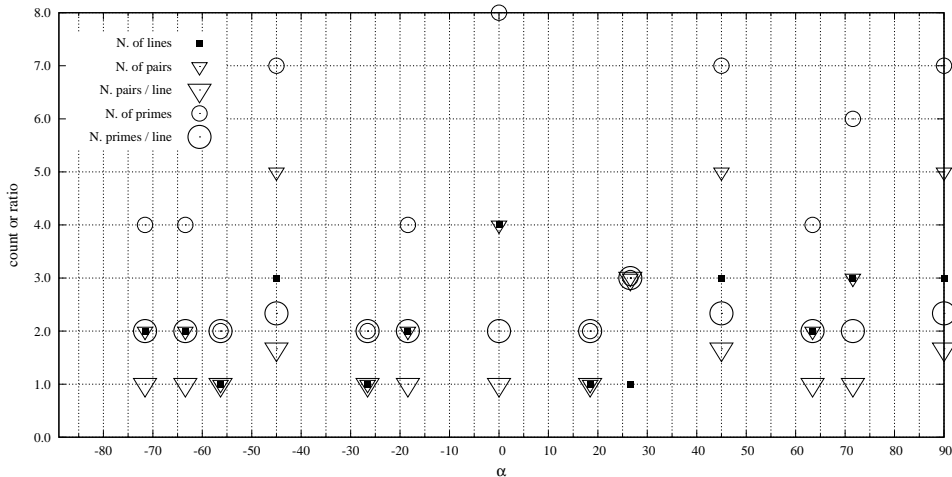
Fig. 5. Listing of the results file for 5×5 Ulam square.

Fig. 6. Numbers of the lines, voting pairs and primes, absolute and per line, versus line direction α for the square of size 5×5 plotted from the data contained in the listing shown in Fig. 5.

References

1959

[1] P.V.C. Hough. Machine analysis of bubble chamber pictures. In *Proc. Int. Conf. on High Energy Accelerators and Instrumentation*. CERN.

1962

[2] P.V.C. Hough. A method and means for recognizing complex patterns. U. S. Patent 3.069.654.

1964

[3] M.L. Stein, S.M. Ulam, and M.B. Wells. A visual display of some properties of the distribution of primes. *The American Mathematical Monthly*, 71(5):516–520. `doi:10.2307/2312588`.

1972

[4] R.D. Duda and P.E. Hart. Use of the Hough transformation to detect lines and curves in pictures. *Comm. Assoc. for Computing Machinery*, 15:11–15. `doi:10.1145/361237.361242`.

1985

[5] R.S. Wallace. A modified Hough transform for lines. In *Proc. IEEE Comput. Soc. Conf. on Comput. Vision and Patt. Recogn. CVPR '85*, pages 665–667, San Francisco, USA.

1988

[6] J. Illingworth and J. Kittler. A survey of the Hough transform. *Comp. Vision, Graph., and Image Proc.*, 44(1):87–116. `doi:10.1016/S0734-189X(88)80033-1`.

1993

[7] V.F. Leavers. Which Hough transform? *CVGIP: Image Understanding*, 58:250–264. `doi:10.1006/ciun.1993.1041`.

2007

[8] H. Rudd. Ulamspiral.com. `ulamspiral.com`.

2004

[9] P. Meer. Robust techniques for computer vision. In G. Medioni and S.B. Kang, editors, *Emerging Topics in Computer Vision*, pages 107–190. Prentice Hall.

2006

[10] L.J. Chmielewski. *Metody akumulacji danych w analizie obrazów cyfrowych*. Akademicka Oficyna Wydawnicza EXIT, Warszawa. `www.lchmiel.pl/akum06`.

2008

[11] D. Antolovic. Review of the Hough transform method, with an implementation of the fast Hough variant for line detection. Department of Computer Science, Indiana University.

Color Transformation Method that Preserves the Impression of Texture in Virtual Makeover System

Joanna Kaczmarczyk, Maciej Pankiewicz

Faculty of Applied Informatics and Mathematics (WZIM)
Warsaw University of Life Sciences (SGGW)
Nowoursynowska 159, 02-775 Warsaw, Poland
`http://www.wzim.sggw.pl`

Abstract. The algorithms of color transformation that preserves the impression of texture are used in virtual makeover systems, where maintaining the impression of unaltered texture is important in the process of transforming the color. The content of this paper covers the process of implementing the algorithm of digital picture color transformation with its main objective – minimizing its influence on the texture structure. The main idea of the presented algorithm is to determine the area in HSV space that consists of the original picture pixels and then, to move it towards the target color in such a way that every color is moved by the same vector, limited only by the fact that the transformation is not always possible. The analysis of the algorithm was conducted based on fragments of real face photographs. Its results were compared on the basis of measures estimated on the run length matrix and the co-occurrence matrix.

Key words: color, texture, color transform, virtual makeover, digital image processing

1. Virtual makeup and color spaces

Picture analysis methods are commonly used in virtual makeup systems, where a camera and screen function as a mirror, in which the process of putting on virtual makeup can be observed in real time. The quality of such applications' functionality depends on the algorithms of image processing and, in particular, their ability to change the color while maintaining the impression of image texture.

The color projection into a digital form is done through mathematical models that enable the description of the color using numeric parameters in coordinate system. The systems that enable this projection as well the descriptions of rules of such projections are color spaces [1, 2, 15, 16, 17, 18, 19]. There are a few different sets of parameters that can describe the same color, thus various color spaces. Two main approaches can be distinguished – sets based on trichromatic color vision theory, modeled on basis of the *physiology of human eyes* and sets in which the information on luminance and chromatic attributes of a color is independent, modeled on the basis of the *human perception of color*. The examples of color spaces are CIE XYZ – created by International Commission on Illumination CIE (fr. *Comission Internationale de l'Eclairage*), CIE RGB, RGB – Red,

Green, Blue (for hardware applications), CMYK – Cyan, Magenta, Yellow, Kontur (for printing applications), HSV – Hue, Saturation, Value, HSL – Hue, Saturation, Lightness and CIE L$\alpha\beta$.

Choice of an optimal color space depends on its use. RGB model works best in applications that use light-emitting devices; HSV arranges the colors in a way that is intuitive for a human being, to simplify the interaction between users and colors; CIE L$\alpha\beta$ is a response to the need for perceptual uniformity of a color space. The decision on selecting the color space for a specific application should not be made hastily, as evidenced by studies on the accuracy of color matching done by users in a system based on RGB and HSV models [20], the results of which did not confirm the superiority of HSV space in the interaction with the user.

2. Color and texture

In the context of computer graphics, it is a great difficulty to provide a clear definition of the concept of texture. The definitions refer, among others, to *repetition of certain segments* of similar appearance and their distribution according to established rules, modeled on texture comparison from digital images to material specific to a particular group of real-world objects and surfaces (wood, sand, wool, etc.), or determined by a "change in the data at a lower level than is currently under consideration" [1, 2, 3, 4, 5, 6, 7, 18]. As there is no mathematical rule that would allow describing any chosen texture, finding the way to represent the textures digitally is one of the fundamental problems in terms of their processing. In addition to this problem there are four basic issues related to classic texture processing:

- *Classification* – identifying the object in the image, based on an analysis of texture that covers it;
- *Segmentation* – dividing the image into areas of different textures;
- *Detection of defects* – the process of deciding whether the texture of the image contains any irregularities;
- *Applying textures* – to objects in the image, in particular to modeled three-dimensional objects [7].

Due to the difficulty in describing the digital representation of texture, it is also problematic to compare them. Most commonly, in the process of comparing similarity of two textures, numerical measures and other parameters (e.g. geometrical) are used, which make it possible to describe the texture in such a way which enables distinguishing it from other textures at a certain level of probability. It relates to both the problem of *extracting* characteristic features of a texture and *selecting* such features that may be useful in the process of distinguishing (classifying) image textures (so-called *discriminative features*). Numerical measures corresponding to these parameters are defined as

descriptors. The methods of texture description can be divided into structural (geometric – where the description of a texture consists of component definitions and the rules of their arrangement) and statistical (probabilistic – where the analysis is conducted at the level of individual pixels and their relations) [1, 2, 3, 4, 5, 6, 7, 8]. Geometrical methods include, among others: Grey Level Co-occurrence Matrix (GLCM) and Run Length Matrix (RLE).

Co-occurrence matrix is a tool to analyze three measures that characterize the texture structure: contrast i, entropy e and linear correlation of data c. Each of these measures belongs to a different group – they measure different features and there are no direct links between them (their values do not depend on one another), so that this collection should be sufficient to determine the characteristic features of every group of sample images.

Homogeneous pixel string matrix [6, 21], although very similar to the measure described above, is based on the analysis of components that form the texture. In this case, the elements considered are chains of pixels forming a single line of the same level of brightness. Run-length matrixes are determined for a given direction of θ (tilt of a chain) – usually: horizontal ($0°$) and vertical ($90°$), as well as two intermediate directions ($45°$ and $135°$). The elements of matrix R_{ij} contain information about how many times does a run of a specific length r and brightness g occur in the image.

Some statistical measures that may be obtained from run-length matrix are, for example, a reverse short run emphasis, long run emphasis, grey level non-uniformity, run-length non-uniformity and fraction of image in runs.

In addition, Pearson's correlation coefficient calculated for a random variable, which is the pixel brightness of two images, will determine the similarity of textures. The main advantage of this method is its independence from data presented in the image. Whatever the situation is, if the coefficient value is the same, it means that the level of similarity of textures will be the same as well.

3. Analysis of color textures

Methods of color texture analysis [2, 3, 9] are directly derived from those used for black and white images. A vast majority of commonly used methods in this field is practically identical for both groups of images. It involves presenting the color texture in greyscale and using tools for black and white image analysis in the processed image. Separating the color from the picture means removing chromatic features from the pixels of the image, leaving only the information about image brightness levels. The black and white texture that remains (understood as the distribution of pixel brightness on the surface of an object) can be further processed in accordance with the principles of tools created for greyscale images. Because texture and color of the objects are strongly related in nature, such treatment of data can be considered as lossy – it loses some information about the

imaged objects. The conclusion is that the results of such analysis of an image may fall on a lower level than when analyzing both characteristics simultaneously. Note, however, that the classification of textures based on greyscale images provides good results.

4. The algorithm of color transformation

The basic premise of the algorithm of color transformation is to preserve the image texture in the most unaltered form possible. For this purpose, it is advised to transfer the colors in an unchanged structure from their color space into a new space, designated by a chosen target color. This way, any interrelationship between source image pixels should be preserved and restored in the image with changed colors.

Of the previously described color spaces it was decided to use the HSV space, abandoning RGB space (due to its lack of intuitiveness in use) and CIE L$\alpha\beta$ (due to a high degree of difficulty of calculations and the need for lossy conversion to RGB space, which could result in additional interferences). The structure of HSV space is the reason why it is often used in different aspects, due to its efficiency in use by color transformation algorithms. The idea of the algorithm created is therefore the designation of an area within HSV space consisting of source image pixels and moving it entirely towards the target color in such a way, that each color is shifted by the same vector, with the constraint that it is not always possible. Only in the case of changing the hue H, the algorithm will work correctly – irrespective of the type of transformation, shifting in the plane will show the correct value of the new parameter, because it forms a circle. Unfortunately, in the case of changes in the intensity S or brightness V, the vector may cause moving the pixels outside the boundaries of the space.

The first possible solution of this problem is to set the maximum values of a parameter, always if it exceeds its maximum, and resetting it if it moves beyond the lower limit of parameter value. The main disadvantage of this solution is the fact that in case of larger fragments of an image that are covered in shadow or in places with strong flares of light, using this method for the brightness parameter would result in the formation of large areas of uniform black and uniform white, respectively. Preserving the impression of the texture is impossible. Therefore, it is necessary to use a different procedure for the parameter V (which most strongly affects the texture).

The best seems to be to use the mechanism of slowing down the changes of obtained color brightness values of the source image, when they come to extreme values. Given the fact that human eye copes better with distinguishing light colors than dark ones, this proximity to extreme values for a centigrade greyscale can be 5 and 10 units for black and white respectively. Thus, if the brightness of the target pixel is less than 5 (especially if it is less than 0), its value would be between 0 and 5, proportionally to the difference between the brightness of the source pixel and minimal brightness of the image. It is the same in the case of the surroundings of a white point. However, because

the texture is to remain unaltered, such smoothing should be done only if it is necessary, that is, when the chosen target color will cause the values to exceed the boundaries of the space.

The second important issue is *the choice of color space point* among those in the source image, for the one that would best characterize the *source* color for transformation. This color is needed to indicate the value of the translation vector which represents the transformation. Due to possible large areas of shadow or flare, it is best to use the average value of colors form the whole transformed image. In the case of using such measures as median or dominant, in extreme cases such deviations could completely undermine the effectiveness of the algorithm by choosing a completely bright or dark color as the point of reference.

Ultimately, the color transformation algorithm is as follows (qualifiers in subscripts are self-explanatory):

- Finding the average color values of the image (c_{avg}) as well as maximum (v_{max}) and minimum (v_{min}) brightness of the image.
- Finding the translation vector for the source color (c_{avg}) and its target (c_{tgt}) form: $W = [(H_{tgt} - H_{avg}), (S_{tgt} - S_{avg}), (V_{tgt} - V_{avg})]$.
- Determining the parameters of the new color for all pixels in the image:
  - hue: $H_{new} = H_{old} + W[H]$, if $H_{new} < 0°$, a full angle should be added to the resulting value; the same for $H_{new} > 360°$ - a full angle should be subtracted from the value;
  - saturation: $S_{new} = S_{old} + W[S]$, if $S_{new} < 0$, then $S_{new} = 0$; if $S_{new} > 100$, then $S_{new} = 100$;
  - brightness (value):
    - if $V_{old} + W[V] < 5$ and $v_{min} + W[V] < 0$, then $V_{new} = 5\frac{V_{old}}{V_5}$, with $V_5 = 5 - W[V]$ (limit value, where slowing down the drop in brightness next to black color starts);
    - if $V_{old} + W[V] > 90$ and $V_{max} + W[V] > 100$, then $V_{new} = 90 + 10\frac{V_{old} - V_{90}}{100 - V_{90}}$, with $V_{90} = 90 - W[V]$ (value, where slowing down the increase of brightness next to white color starts);
    - otherwise $V_{new} = V_{old} + W[V]$.

5. Solution implementation

In virtual makeup systems [10, 11, 12, 13, 14] the analysis is usually subjected to two separate aspects: face recognition, and more specifically identifying its parts, and color transformation, i.e. applying makeup. This study describes the mechanism of color transformation with the purpose of changing the color in the image and does not analyze the issue of face recognition. Since the transfer of cosmetics is a specialized process, the algorithms used in these systems are not commonly used in other areas. There are also

Tab. 1. The results of the algorithm on images of the facial skin.

Image	Transformation I	Transformation II	Transformation III
	$e = 3{,}092$ $p = 0{,}992$	$e = 14{,}473$ $p = 0{,}969$	$e = 21{,}98$ $p = 0{,}435$
	$e = 0{,}312$ $p = 0{,}989$	$e = 5{,}861$ $p = 0{,}972$	$e = 14{,}362$ $p = 0{,}355$
	$e = 0{,}601$ $p = 0{,}981$	$e = 11{,}064$ $p = 0{,}922$	$e = 5{,}491$ $p = 0{,}692$
	$e = 0{,}419$ $p = 0{,}925$	$e = 2{,}821$ $p = 0{,}823$	$e = 10{,}66$ $p = 0{,}341$
	$e = 2{,}266$ $p = 0{,}975$	$e = 18{,}7$ $p = 0{,}888$	$e = 13{,}453$ $p = 0{,}598$
	$e = 0{,}913$ $p = 0{,}967$	$e = 6{,}212$ $p = 0{,}826$	$e = 8{,}472$ $p = 0{,}712$

not many sources form which ideas and solutions can be drawn and a little number of publications on this type of color transfer exist.

The analysis of results generated by the algorithm was conducted for two characteristic surfaces on a face – the skin on cheeks (Tab. 1) and lips (Tab. 2). Each group is represented by six samples. For each sample the transformations performed were:

- a slight change of color – the target color is similar to the original one; gentle color, with weak features (Transformation I);
- change of brightness – target color is characterized by a high value of parameter V (Transformation II);
- change of intensity and hue – target color of an entirely different hue, darker and with high intensity (Transformation III).

In the analysis of values of the Pearson correlation coefficient p, a distinct influence of the modification of basic algorithm rules (resulting from the target values exceeding the acceptable ranges for HSV space) on the obtained results can be observed. The largest decrease in correlation was when a relatively homogeneous structure of the facial skin was also "flattened" by assigning the same value of intensity to a large number of

Tab. 2. The results of the algorithm on images of lips.

Image	Transformation I	Transformation II	Transformation III
	$e = 10{,}697$ $p = 0{,}997$	$e = 6{,}9568$ $p = 0{,}987$	$e = 15{,}279$ $p = 0{,}739$
	$e = 5{,}096$ $p = 0{,}997$	$e = 28{,}43$ $p = 0{,}986$	$e = 30{,}14$ $p = 0{,}593$
	$e = 16{,}877$ $p = 0{,}995$	$e = 34{,}809$ $p = 0{,}99$	$e = 15{,}279$ $p = 0{,}739$
	$e = 16{,}816$ $p = 0{,}993$	$e = 35{,}773$ $p = 0{,}981$	$e = 31{,}109$ $p = 0{,}65$
	$e = 7{,}07$ $p = 0{,}996$	$e = 3{,}42$ $p = 0{,}983$	$e = 26{,}046$ $p = 0{,}926$
	$e = 43{,}246$ $p = 0{,}998$	$e = 65{,}823$ $p = 0{,}99$	$e = 67{,}895$ $p = 0{,}904$

pixels. This took place during Transformation III, because many pixel colors of the target image exceeded the maximum value of S parameter, which resulted in assigning a constant (maximum) value to them.

In other cases, the correlation between images is very high, especially in Transformation I. This conversion shows the situation in which the algorithm performs the color shift with the space in an almost unaltered configuration. There were no issues of exceeding the borders of the space. Therefore, there was no need for additional manipulation of brightness and saturation of color, which means that the differences between the color parameters are constant for each pair of corresponding image pixels. The correlation coefficient, however, is indicated for the image in greyscale. Because it is designated in accordance with the human perception (not based on parameter V itself), even such a direct transformation affects the perceived texture appearance.

The results obtained by the method of co-occurrence matrix e can not be compared in the same way, because their values strongly depend on the type of a presented image and must be considered in a broader context. However, when analyzing individual image samples, and keeping in mind the good results of using this method in texture

classification, it should be noted that despite a substantial deformation of textures in Transformation III (where Pearson's correlation coefficient does not indicate a significant similarity with the original images), they are classified as more alike than the ones obtained in Transformation II (in spite of a high correlation of target and source textures).

Transformations II and III were selected in such a way that they present the critical points of the algorithm, i.e. those in which it is particularly exposed to texture deformations. In fact, such deformation can be observed both in obtained comparison results and in the presented output images. It should be noted, however, that these are extreme cases. Furthermore, these transformations did not lead to deformations, only to equalizing the surface structures. This makes it possible therefore to claim that the created solution conforms to the intent – the impression of texture is preserved.

6. Conclusion

The primary purpose of the algorithm of changing the texture colors is to minimize the loss of information about its structure (appearance). It is crucial in the case of virtual makeup, for the areas where cosmetics are applied not to look artificial. Based on the determined similarity measures, it was confirmed that the algorithm conforms to this intent. However, the primary objective of the virtual makeup system is the resulting visual effect. Therefore, in order to further develop the application, it is necessary to connect this tool to other components that form the virtual makeup system.

It should be noted that the proposed algorithm of transformation leads to flare effects when choosing the target color that is brighter than the original one. Although this effect is desired for some cosmetics (e.g. lip gloss), usually it is expected to bring the opposite effect (matting). Therefore, a modification of the algorithm to allow the manipulation of brightness parameter should be considered, to adapt it to the characteristics of the cosmetic. The structure of the algorithm allows for such modifications, because all the parameters of color channels, including their brightnesses, are processed separately.

References

2005
[1] T. Acharya, A.K. Ray. *Image processing: Principles and applications*. John Wiley & Sons.
2002
[2] R.C. Gonzalez, R.E. Woods. *Digital image processing*. Prentice Hall.
2008
[3] M. Mirmehdi, X. Xie, J. Suri. *Handbook of texture analysis*. Imperial College Press.
2002
[4] M.S. Nixon, A.S. Aguado. *Feature extraction and image processing*. Newnes.
2006
[5] M. Petrou, P.G. Sevilla. *Image Processing. Dealing with textures*. John Wiley & Sons.
1979
[6] R.M. Haralick. Statistical and structural approaches to texture. *Proc. of IEEE*.

1998

[7] M. Tuceryan, A.K. Jain. Texture Analysis. in: C.H. Chen, L.F. Pau, P. S. P. Wang (Eds.) *Handbook of pattern recognition and computer vision*, vol. 2. World Scientific Publishing.

1998

[8] A. Materka A, M. Strzelecki. *Texture Analysis Methods – A Review*. Technical University of Lodz, Institute of Electronics, COST B11 Report, Brussels.

2001

[9] A. Drimbarean, P.F. Whelan. Experiments in colour texture analysis. *Pattern Recognition Letters*, vol. 22, no. 10.

2009

[10] A. Dhall et al. Adaptive digital makeup. *Proc. the 5th International Symposium on Advances in Visual Computing*. Part II.

2009

[11] D. Gou, T. Sim. Digital face makeup by example. *IEEE Conference on Computer Vision and Pattern Recognition*.

2007

[12] W.S. Tong et al. Example-based cosmetic transfer. *Proceedings of the 15th Pacific Conference on Computer Graphics and Applications*.

2003

[13] N. Tsumura et al. Image-based skin color and texture analysis/synthesis by extracting hemoglobin and melanin information in the skin. *ACM SIGGRAPH 2003 Papers*.

2010

[14] A.I. Mecwan, V.G. Savani. Virtual makeover using MATLAB. *Int. J. Advancements in Technology*, vol. 1, no. 2.

2005

[15] M.K. Agoston. *Computer graphics and geometric modeling: Implementation and algorithms*. Springer.

1995

[16] J.D. Foley et al. *Wprowadzenie do grafiki komputerowej*. Wydawnictwo Naukowo-Techniczne.

2003

[17] R.G. Kuehni. *Color space and its divisions: Color order from antiquity to the present*. John Wiley & Sons.

2007

[18] W.K. Pratt. *Digital image processing*. Vol. 4. John Wiley & Sons.

2001

[19] G. Paschos. Perceptually uniform color spaces for color texture analysis: an empirical evaluation. *IEEE Trans. Image Processing*, vol. 10, no. 6.

1996

[20] S. Douglas, T. Kirkpatrick. Do color models really make a difference? *Proc. CHI Conference on Human Factors in Computing Systems*.

2011

[21] S. Selvarajah, S.R. Kodituwakku. Analysis and comparison of texture features for content based image retrieval. *Int. J. Latest Trends in Computing*, vol. 2, no. 1.